Available online at www.sciencedirect.com
SCIENCE DIRECT®
Journal of Sound and Vibration 268 (2003) 305–321
JOURNAL OF SOUND AND VIBRATION
www.elsevier.com/locate/jsvi

An actuator for the $n = 2$ circumferential mode of a pipe

W. Variyart, M.J. Brennan*

The Institute of Sound and Vibration Research, University of Southampton, Southampton SO17 1BJ, UK

Received 20 June 2002; accepted 14 November 2002

Abstract

The axial propagating wave of the $n = 2$ circumferential mode in a pipe can cause large vibration when the wave cuts on and may cause fatigue damage or transmit structure-borne noise along the pipe. For this reason, a control system (passive or active) is desirable. In this paper, a PZT modal actuator for the $n = 2$ mode, which could be used in an active control system, is described. It is constructed from a set of PZT elements bonded to the pipe. By arranging them in form of the $n = 2$ mode, only the motion of that particular mode is generated and is proportional to the applied voltage. With two PZT modal actuators, which are in forms of sine and cosine functions, the orientation of the propagating wave of the $n = 2$ mode can be modified to any angle. In this paper a theoretical model for the actuator is developed and is validated by some experimental work.

1. Introduction

In recent years, the application of piezoelectric actuators for active vibration control has been increasing due to the property of piezoelectric material in that it is able to convert electrical to mechanical energy. In addition, it is relatively lightweight, can be tailored into shapes [1], and can be readily integrated into a structure without grossly changing the mechanical properties of the system. However, the main problem for single-channel control systems is that of spillover [2], which is the effect of the unobserved and uncontrolled modes. This effect will degrade the performance of the control system. To avoid this problem, a modal actuator can be employed to selectively actuate the vibration of a particular mode. A modal actuator can be made by shaping a piezoelectric material into the shape of the mode needed to be actuated.

Two commercially available types of piezoelectric materials are lead zirconate titanate (PZT) and polyvinylidene fluoride (PVDF). Because it is easily shaped, much effort has been

*Corresponding author.
E-mail address: mjb@isvr.soton.ac.uk (M.J. Brennan).

0022-460X/03/$ - see front matter
doi:10.1016/S0022-460X(03)00253-0

concentrated on developing PVDF as a modal actuator. Such applications on beams and plates have been reported by Burke and Hubbard, Jr [3], Lee [4] and Lee and Moon [5], and on pipes by Tzou [6] and Sung et al. [7]. However, this type of piezoelectric material is not very suitable for many actuator applications as discussed by Brennan et al. [8]. This is because it has relatively low stiffness, which does not facilitate effective mechanical coupling to the structure, and small dielectric constant (d_{31}), which implies that it needs a high applied voltage as reported by Tani et al. [9] and Qiu and Tani [10]. Having high stiffness and high dielectric constant, PZT is more appropriate for actuator applications. Such applications on a finite pipe have been described Lester and Lefebvre [11] and Lalande et al. [12]. They used a pair of PZT elements bonded on the opposite sides of the pipe (inside and outside) to generate a pure moment and a pure in-plane force. However, in both pieces of work the actuator was not a modal actuator, and in reality it is difficult to locate the PZT elements on both sides (inside and outside) of a pipe.

In this paper, the design of a PZT modal actuator for a thin-walled pipe is described. An analytical model that relates the voltage applied to the modal actuator to the dynamic behaviour of an infinitely long pipe is developed. Before this can be done, however, the transfer function relating the radial displacement of the pipe to the excitation voltage applied to a single PZT element has to be derived. Once this has been done a modal actuator can be designed using a number of elements. To validate the model some experimental work is also conducted.

2. Excitation by a single PZT element

The co-ordinate system for an infinite *in-vacuo* pipe of mid-surface radius a and wall thickness h is shown in Fig. 1(a), where w, v and u are the radial, tangential and axial pipe displacements

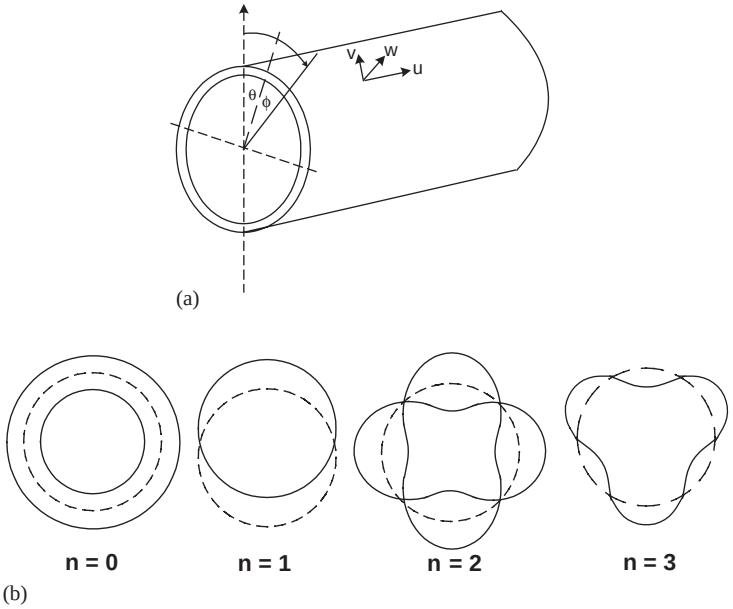

Fig. 1. Cylindrical co-ordinate system and mode shapes of a pipe.

respectively, θ is the azimuthal angle and ϕ is a reference angle clockwise from the vertical. Because of the closure of the pipe in the circumferential direction, the mode-shapes in this direction take the form of sine or cosine functions. The first four modes are illustrated in Fig. 1(b), where n denotes the modal order, which conventionally starts at $n = 0$; n also denotes the integer number of circumferential wavelengths that fit into the circumference of the pipe at the cut-on frequency of the nth mode. For each mode, there are eight axial waves, four are right-going and four are left-going. The characteristics of these waves are described in Refs. [13,14].

Fig. 2 depicts a single PZT element bonded to the outer layer of a pipe. When a voltage is applied, it will generate in-plane forces, q_s and q_θ, and moments, m_s and m_θ, in the axial and circumferential directions respectively [15]. These forces and moments simultaneously excite the pipe, and the equations of motion can be formulated by considering the force and moment equilibrium of the pipe element as follows [16]

$$\frac{\partial(N_s - q_s)}{\partial s} + \frac{\partial N_{\theta s}}{\partial \theta} - \rho a h \frac{\partial^2 u}{\partial t^2} = 0,$$
$$\frac{\partial(N_\theta - q_\theta)}{\partial \theta} + \frac{\partial N_{s\theta}}{\partial s} + Q_\theta - \rho a h \frac{\partial^2 v}{\partial t^2} = 0,$$
$$(N_\theta - q_\theta) - \frac{\partial Q_s}{\partial s} - \frac{\partial Q_\theta}{\partial \theta} + \rho a h \frac{\partial^2 w}{\partial t^2} = 0,$$
$$\frac{\partial(M_s - m_s)}{\partial s} + \frac{\partial M_{\theta s}}{\partial \theta} - a Q_s = 0,$$
$$\frac{\partial(M_\theta - m_\theta)}{\partial \theta} + \frac{\partial M_{s\theta}}{\partial s} - a Q_\theta = 0, \qquad \text{(1a-e)}$$

where ρ is the density of the pipe, $s = x/a$ is the non-dimensional axial distance along the pipe, $N_s, N_\theta, N_{\theta s}, N_{s\theta}, Q_s, Q_\theta$, and $M_s, M_\theta, M_{\theta s}, M_{s\theta}$ are internal forces and moments. By substituting Q_s, Q_θ, from Eqs. 1(d) and (e) into Eqs. 1(b) and (c) and using Flügge's shell theory [17] to express the internal forces and moments in terms of the pipe deformation, the equations of pipe motion

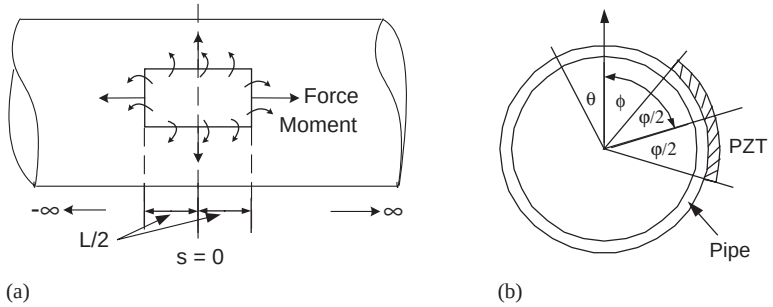

Fig. 2. A PZT element bonded to an infinite pipe; (a) Axial direction, (b) cross-section of the structure showing the co-ordinate system.

(Eqs. (1a–e)) can be written in matrix form as follows

$$\begin{bmatrix} A_{11} & A_{12} & A_{13} \\ A_{21} & A_{22} & A_{23} \\ A_{31} & A_{32} & A_{33} \end{bmatrix} \begin{bmatrix} u(s,\theta,t) \\ v(s,\theta,t) \\ w(s,\theta,t) \end{bmatrix} = \frac{a}{K} \begin{bmatrix} \dfrac{\partial q_s}{\partial s} \\ \dfrac{\partial m_\theta}{a\partial\theta} + \dfrac{\partial q_\theta}{\partial\theta} \\ q_\theta - \dfrac{1}{a}\dfrac{\partial^2 m_s}{\partial s^2} - \dfrac{1}{a}\dfrac{\partial^2 m_\theta}{\partial\theta^2} \end{bmatrix}, \tag{2}$$

where

$$A_{11} = \left(\frac{\partial^2}{\partial s^2} + \frac{(1-v)}{2}(1+\beta^2)\frac{\partial^2}{\partial\theta^2} - \frac{\rho(1-v^2)a^2}{E}\frac{\partial^2}{\partial t^2}\right)$$

$$A_{12} = \left(\frac{(1+v)}{2}\frac{\partial^2}{\partial s\partial\theta}\right), \quad A_{13} = \left(v\frac{\partial}{\partial s} - \beta^2\frac{\partial^3}{\partial s^3} + \beta^2\frac{(1-v)}{2}\frac{\partial^3}{\partial s\partial\theta^2}\right), \quad A_{21} = A_{12},$$

$$A_{22} = \left(\frac{(1-v)}{2}(1+3\beta^2)\frac{\partial^2}{\partial s^2} + \frac{\partial^2}{\partial\theta^2} - \frac{\rho(1-v^2)a^2}{E}\frac{\partial^2}{\partial t^2}\right), \quad A_{23} = \left(\frac{\partial}{\partial\theta} - \beta^2\frac{(3-v)}{2}\frac{\partial^3}{\partial s^2\partial\theta}\right),$$

$$A_{31} = A_{13}, \quad A_{32} = A_{23}, \quad A_{33} = \left(1 + \beta^2\nabla^4 + \beta^2 + 2\beta^2\frac{\partial^2}{\partial\theta^2} + \frac{\rho(1-v^2)a^2}{E}\frac{\partial^2}{\partial t^2}\right),$$

$$\nabla^4 = \frac{\partial^4}{\partial s^4} + \frac{\partial^4}{\partial\theta^4} + \frac{\partial^4}{\partial s^2\partial\theta^2},$$

$K = Eh/(1-v^2)$ is the membrane stiffness, $\beta = h/a\sqrt{12}$, E and v are Young's modulus and Poisson ratio of the pipe, respectively.

To develop Eq. (2), the displacements, applied forces and applied moments are transformed to the wavenumber domain. Using the Fourier transform, the displacements of a pipe can be written as [18]

$$u(s,\theta,t) = \frac{1}{2\pi}\int_{-\infty}^{\infty}\sum_{n=0}^{\infty}\varepsilon_n\overline{U_n(\hat{k}_n)}\cos(n\theta)e^{j(\hat{k}_n s - \pi/2 - \omega t)}\,d\hat{k}_n,$$

$$v(s,\theta,t) = \frac{1}{2\pi}\int_{-\infty}^{\infty}\sum_{n=0}^{\infty}\varepsilon_n\overline{V_n(\hat{k}_n)}\sin(n\theta)e^{j(\hat{k}_n s - \omega t)}\,d\hat{k}_n,$$

$$w(s,\theta,t) = \frac{1}{2\pi}\int_{-\infty}^{\infty}\sum_{n=0}^{\infty}\varepsilon_n\overline{W_n(\hat{k}_n)}\cos(n\theta)e^{j(\hat{k}_n s - \omega t)}\,d\hat{k}_n, \tag{3a-c}$$

where n is the circumferential mode number, $\varepsilon_n = 1$ for $n = 0$ and $\varepsilon_n = 2$ for $n \geqslant 1$, $\hat{k}_n$ is the non-dimensional axial wavenumber of the nth mode (the axial wavenumber multiplied by the radius of the pipe), ω is the angular frequency, $\overline{U_n(\hat{k}_n)}$, $\overline{V_n(\hat{k}_n)}$ and $\overline{W_n(\hat{k}_n)}$ are the axial, tangential and radial pipe displacements of the nth mode in the wavenumber domain, respectively.

In the dynamic model, the excitation forces, q_s and q_θ, and moments, m_s and m_θ, are assumed to be uniform over the PZT surface [19] and can be represented by the unit step function as follows (omitting terms of $e^{-j\omega t}$ for simplicity).

$$\begin{aligned} q_s &= q_{s0}[H(s-L_a)-H(s+L_a)][H(\theta-\varphi)-H(\theta+\varphi)],\\ q_\theta &= q_{\theta0}[H(s-L_a)-H(s+L_a)][H(\theta-\varphi)-H(\theta+\varphi)],\\ m_s &= m_{s0}[H(s-L_a)-H(s+L_a)][H(\theta-\varphi)-H(\theta+\varphi)],\\ m_\theta &= m_{\theta0}[H(s-L_a)-H(s+L_a)][H(\theta-\varphi)-H(\theta+\varphi)], \end{aligned} \tag{4a-d}$$

where $q_{s0}, q_{\theta0}$, and $m_{s0}, m_{\theta0}$ are the static forces and moments generated by the PZT element in the axial and circumferential directions, respectively, $L_a = L/2a$ is the non-dimensional length of the PZT, L is the length of the PZT and H is the unit step function, which can be expressed in the term of the delta function δ [20]

$$H(s-s_0) = \int_{-\infty}^{s-s_0} \delta(s_i)\,\mathrm{d}s_i. \tag{5}$$

The delta functions of $\delta(s-L_a)$ and $\delta(\theta-\varphi)$ may be expressed as

$$\delta(s) = \frac{1}{2\pi}\int_{-\infty}^{\infty} e^{j\hat{k}_n(s-L_a)}\,\mathrm{d}\hat{k}_n \quad \text{and} \quad \delta(\theta-\varphi) = \frac{1}{2\pi}\sum_{n=-\infty}^{\infty} e^{jn(\theta-\varphi)}. \tag{6a, b}$$

By substituting for the delta function from Eq. (6) into Eq. (5), the differences between the unit step functions at the edges of the PZT in the axial and circumferential directions can be written as

$$\begin{aligned} H(s-L_a)-H(s+L_a) &= -\frac{1}{\pi}\int_{-\infty}^{\infty}\frac{1}{\hat{k}_n}\sin(\hat{k}_nL_a)e^{jk_as}\,\mathrm{d}\hat{k}_n,\\ H(\theta-\varphi)-H(\theta+\varphi) &= -\frac{1}{\pi}\sum_{n=0}^{\infty}\frac{\varepsilon_n}{n}\sin(n\varphi)\cos(n\theta). \end{aligned} \tag{7a, b}$$

Substituting for the displacements given in Eq. (3), and for the forces and moments given in Eq. (4) with the unit step function from Eq. (7) into Eq. (2) yields

$$\begin{bmatrix} L_{11} & L_{12} & L_{13}\\ L_{21} & L_{22} & L_{23}\\ L_{31} & L_{32} & L_{33} \end{bmatrix} \begin{bmatrix} \overline{U_n(\hat{k}_n)}\\ \overline{V_n(\hat{k}_n)}\\ \overline{W_n(\hat{k}_n)} \end{bmatrix} = -\frac{a}{K}\sin(n\varphi)\sin(\hat{k}_nL_a) \begin{bmatrix} \dfrac{2}{n\pi}q_{s0}\\ \dfrac{2}{\hat{k}_n\pi}\left(\dfrac{m_{\theta0}}{a}+q_{\theta0}\right)\\ \dfrac{2}{a\pi}\left(\dfrac{a}{n\hat{k}_n}q_{\theta0}+\dfrac{\hat{k}_n}{n}m_{s0}+\dfrac{n}{\hat{k}_n}m_{\theta0}\right) \end{bmatrix}, \tag{8}$$

where

$$L_{11} = \hat{k}_n^2 + \frac{(1-\nu)}{2}(1+\beta^2)n^2 - \Omega^2, \quad L_{12} = \frac{(1+\nu)}{2}n\hat{k}_n,$$

$$L_{13} = \nu\hat{k}_n + \beta^2\hat{k}_n^3 - \frac{(1-\nu)}{2}\beta^2n^2\hat{k}_n, \quad L_{21} = L_{12},$$

$$L_{22} = \frac{(1-v)}{2}(1+3\beta^2)\hat{k}_n^2 + n^2 - \Omega^2, \quad L_{23} = n + \frac{(3-v)}{2}\beta^2 n\hat{k}_n^2,$$

$$L_{31} = L_{13}, \quad L_{32} = L_{23}, \quad L_{33} = 1 + \beta^2 + \beta^2(\hat{k}_n^2 + n^2)^2 - 2\beta^2 n^2 - \Omega^2.$$

Inverting the matrix $\mathbf{L}$, the amplitudes of the displacements can be written as

$$\begin{bmatrix} \overline{U_n(\hat{k}_n)} \\ \overline{V_n(\hat{k}_n)} \\ \overline{W_n(\hat{k}_n)} \end{bmatrix} = -2\frac{a}{\pi K}\sin(n\varphi)\sin(\hat{k}_n L_a) \begin{bmatrix} I_{11} & I_{12} & I_{13} \\ I_{21} & I_{22} & I_{23} \\ I_{31} & I_{32} & I_{33} \end{bmatrix} \begin{bmatrix} \frac{1}{n} q_{s0} \\ \frac{1}{\hat{k}_n}\left(\frac{m_{\theta 0}}{a} + q_{\theta 0}\right) \\ \frac{1}{a}\left(\frac{a}{n\hat{k}_n} q_{\theta 0} + \frac{\hat{k}_n}{n} m_{s0} + \frac{n}{\hat{k}_n} m_{\theta 0}\right) \end{bmatrix}, \quad (9)$$

where $\mathbf{I}$ is the inverse matrix of $\mathbf{L}$. The radial displacement in the wavenumber domain is given by

$$\overline{W_n(\hat{k}_n)} = -\frac{2a}{\pi K}\sin(n\varphi)\sin(\hat{k}_n L_a) \times \left[\left(\frac{q_{s0}}{n} I_{31} + \frac{q_{\theta 0}}{\hat{k}_n} I_{32} + \frac{q_{\theta 0}}{n\hat{k}_n} I_{33}\right) + \frac{1}{a\hat{k}_n}(I_{32} + nI_{33}) m_{\theta 0} + \frac{\hat{k}_n}{an} I_{33} m_{s0}\right], \quad (10)$$

where $I_{31}(\hat{k}_n) = (L_{21}L_{32} - L_{22}L_{31})_n/|\mathbf{L}|_n$, $I_{32}(\hat{k}_n) = (L_{12}L_{31} - L_{11}L_{32})_n/|\mathbf{L}|_n$ and

$$I_{33}(\hat{k}_n) = (L_{11}L_{22} - L_{12}L_{21})_n/|\mathbf{L}|_n \quad (11)$$

As described by Variyart [15], the relationship between the induced forces and the induced moments in the pipe to the voltage applied to the PZT element, V, are $q_{s0} = q_{\theta 0} = g_q V$, $m_{s0} = m_{\theta 0} = g_m V$, where g_q and g_q are the static gains of the PZT element generating the forces and moments respectively. Substituting these relations into Eq. (10) gives

$$\overline{W_n(\hat{k}_n)} = -\frac{2a}{\pi K}\frac{\sin(n\varphi)\sin(\hat{k}_n L_a) g_q V}{n\hat{k}_n}\left[(\hat{k}_n I_{31} + nI_{32} + I_{33}) + (nI_{32} + (n^2 + \hat{k}_n^2) I_{33})\frac{g_m}{a g_q}\right]. \quad (12)$$

Omitting terms of $e^{-j\omega t}$ for simplicity, the radial displacement for a particular mode in the frequency domain is obtained by substituting Eq. (12) into Eq. (3c) to give

$$W_n(s,\theta) = -\frac{a\varepsilon_n}{\pi^2 K}\cos(n\theta)\int_{-\infty}^{\infty}\frac{\sin(n\varphi)\sin(\hat{k}_n L_a) g_q V}{n\hat{k}_n} \times \left[(\hat{k}_n I_{31} + nI_{32} + I_{33}) + (nI_{32} + (n^2 + \hat{k}_n^2) I_{33})\frac{g_m}{a g_q}\right] \mathrm{d}\hat{k}_n. \quad (13)$$

Assuming that $n\varphi \ll 1$ and $\hat{k}_n L_a \ll 1$, then $\sin(n\varphi) \cong n\varphi$ and $\sin(\hat{k}_n L_a) \cong \hat{k}_n L_a)$, respectively and the amplitude of the radial displacement becomes

$$W_n(s,\theta) = -\frac{a\varepsilon_n \varphi L_a g_q V}{\pi^2 K}\cos(n\theta)\int_{-\infty}^{\infty}\left[(\hat{k}_n I_{31} + nI_{32} + I_{33}) + (nI_{32} + (n^2 + \hat{k}_n^2) I_{33})\frac{g_m}{a g_q}\right] \mathrm{d}\hat{k}_n. \quad (14)$$

As discussed in Refs. [13,14], $|\mathbf{L}|_n$ in Eq. (11) can be expressed as $|\mathbf{L}|_n = \prod_{b=1}^{8}(\hat{k}_n - \hat{k}_{nb})$, where $\hat{k}_{nb}$ is the wavenumber solution of the pipe for the nth mode and is frequency dependent. So, for each frequency, there are eight poles (wavenumbers) at $\hat{k}_n = \hat{k}_{nb}$, and simplified expressions for these are given in Appendix A. The integral can be evaluated using residue theory [20]. Only four poles need to be evaluated, which means that only the waves in the positive direction are taken into account. However, because of the symmetry, the solutions for the waves in the negative direction are the same. The solution to Eq. (14) can be expressed as [20]

$$W_n(s,\theta) = -\mathrm{j}\frac{2a\varepsilon_n\varphi L_a g_q V}{\pi K}\cos(n\theta)\sum_{b=0}^{4}\mathrm{Res}_{nb}\mathrm{e}^{\mathrm{j}\hat{k}_{nb}s}, \tag{15}$$

where

$$\mathrm{Res}_{nb} = \left[(\hat{k}_{nb}I_{31}^r + nI_{32}^r + I_{33}^r) + (nI_{32}^r + (n^2+\hat{k}_{nb}^2)I_{33}^r)\frac{g_m}{ag_q}\right],$$

$$I_{31}^r(\hat{k}_{nb}) = (L_{21}L_{32} - L_{22}L_{31})_{nb}/|\mathbf{L}|'_{nb}, \quad I_{32}^r(\hat{k}_{nb}) = (L_{12}L_{31} - L_{11}L_{32})_{nb}/|\mathbf{L}|'_{nb},$$

$$I_{33}^r(\hat{k}_{nb}) = (L_{11}L_{22} - L_{12}L_{21})_{nb}/|\mathbf{L}|'_{nb}, \quad |\mathbf{L}|'_{nb} = \frac{\partial|\mathbf{L}|_{nb}}{\partial\hat{k}_{nb}}.$$

It should be noted that in the development of the expression for the radial displacement of the nth mode, the orientation has been taken to be zero for simplicity. The radial motion of the pipe in general form can be determined by substituting for θ with $(\theta - \phi)$ to give

$$W(s,\theta) = -\mathrm{j}\frac{2a\varphi L_a g_q V}{\pi K}\sum_{n=0}^{\infty}\sum_{b=1}^{4}\varepsilon_n\cos[n(\theta-\phi)]\mathrm{Res}_{nb}\,\mathrm{e}^{\mathrm{j}\hat{k}_{nb}s}. \tag{16}$$

Finally, the transfer function between the voltage applied to the PZT element and the radial velocity of the pipe is given by

$$T_z = -\mathrm{j}\omega\frac{W(s,\theta)}{V} = -\omega\frac{2a\varphi L_a g_q}{\pi K}\sum_{n=0}^{\infty}\varepsilon_n\cos[n(\theta-\phi)]\sum_{b=1}^{4}\mathrm{Res}_{nb}\mathrm{e}^{\mathrm{j}\hat{k}_{nb}s}. \tag{17}$$

3. $n = 2$ modal actuator

A single PZT element generates radial motion of all modes as shown in Eq. (17). To generate only the radial displacement of the desired mode, a set of PZT elements is required. Arranged in the form of such a mode, it can force the pipe to vibrate only in the desired mode and hence is called a modal actuator.

Excited by a single PZT element, the radial motion obtained from Eq. (17) is a function of three separate parameters, ϕ, θ and s. The radial motion, W, at an angle ϕ_p may be rewritten in a

simple form as

$$W(\phi_p) = V\sum_{n=0}^{\infty} A_n \cos[n(\theta - \phi_p)], \tag{18}$$

where

$$A_n = -\mathrm{j}\frac{2a\varphi L_a \varepsilon_n g_q}{\pi K}\sum_{b=1}^{4} \mathrm{Res}_{nb} \mathrm{e}^{\mathrm{j}\hat{k}_{nb}s}.$$

The sine and cosine functions have the property of orthogonality over a series of discrete, equally spaced points [20]. By applying this property to the above expression, the radial motion of a particular mode can be derived. A set of PZT elements can be arranged to satisfy the discrete orthogonality condition. They are positioned around the pipe with equal angle of $\phi = 0, 2\pi/N, 4\pi/N, \ldots, 2\pi$, where N is the number of circumferential positions or the number of PZT elements. The angle interval between the positions of the PZT elements is $\phi_p = 2\pi(p_z/N)$, where p_z is the circumferential position of the PZT element on the pipe. Substituting for the discrete angle, ϕ_p, into Eq. (18) multiplying by $\cos(2\pi m p_z/N)$ and summing over all of the PZT elements, gives the radial response of the cosine modal actuator, W^c, for the mth mode as

$$\begin{aligned} W^c &= \sum_{p_z=0}^{N-1} W(\phi_p)\cos\left(2\pi m\frac{p_z}{N}\right) \\ &= V^c\sum_{p_z=0}^{N-1}\sum_{n=0}^{\infty} A_n\left[\cos(n\theta)\cos\left(2\pi n\frac{p_z}{N}\right) + \sin(n\theta)\sin\left(2\pi n\frac{p_z}{N}\right)\right]\cos\left(2\pi m\frac{p_z}{N}\right). \end{aligned} \tag{19}$$

With the assumption of N tending to infinity, applying the property of orthogonality gives

$$\begin{aligned} W^c &= \sum_{p_z=0}^{N-1} V_r^c \sum_{n=0}^{\infty} A_n \cos\left[n(\theta - 2\pi n\frac{p_z}{N})\right] \\ &= \begin{cases} \dfrac{1}{2}NV^c A_m\cos(m\theta), & m \neq 0 \text{ or } m \neq \dfrac{N}{2}, \\ NV^c A_m\cos(m\theta), & m = 0 \text{ or } m = \dfrac{N}{2}, \end{cases} \end{aligned} \tag{20}$$

where $V_r^c = V^c\cos\left(2\pi m(p_z/N)\right)$ is the required voltage for the cosine modal actuator. However, when N is finite, there is spillover to the modes greater than $N/2$. It can be seen in Eq. (20) that the required voltage for the cosine modal actuator has to be varied as the cosine function of the position of the PZT elements and the desired mode. For the sine function, the positions of the PZT elements around the pipe are given by $\phi = \pi/N, 3\pi/N, \ldots, (2N-1)/N\,\pi$. The angle of interval between the positions of the PZT for a sine modal actuator is $\phi_p = 2\pi/N\left(p_z + \frac{1}{2}\right)$. Similar to the analysis of the cosine modal actuator, the radial response of the sine modal actuator for the

mth mode is given by

$$W^s = \sum_{p_z=0}^{N-1} V_r^s \sum_{n=0}^{\infty} A_n \cos\left[n\left(\theta - 2\pi n \frac{p_z}{N}\right)\right]$$
$$= \begin{cases} \frac{1}{2} N V^s A_m \sin(m\theta), & m \neq 0 \text{ or } m \neq \frac{N}{2}, \\ N_e V^s A_m \sin(m\theta), & m = \frac{N}{2}, \\ 0, & m = 0, \end{cases} \tag{21}$$

where

$$V_r^s = V^s \sin\left[\frac{2\pi m}{N}\left(p_z + \frac{1}{2}\right)\right]$$

is the required voltage for the sine modal actuator.

Eqs. (20) and (21) imply that the minimum number of the PZT elements required to form the cosine or sine modal actuator are $N = 2$ m. With $N > 2$ m, where $m \geqslant 1$, the total radial response obtained from both sine and cosine modal actuator is given by

$$W^{tot} = \frac{1}{2} N A_m [V^s \sin(m\theta) + V^c \cos(m\theta)]. \tag{22}$$

By letting $V^s = V^{tot} \sin(m\phi_{no})$ and $V^c = V^{tot} \cos(m\phi_{no})$, where $V^{tot} = \sqrt{(V^s)^2 + (V^c)^2}$ is the total voltage supplied to the modal actuator, and $\phi_{no} = 1/m \tan^{-1}(V^s/V^c)$ is the orientation angle relative to the cosine modal actuator, Eq. (22) becomes

$$W^{tot} = \frac{1}{2} N V^{tot} A_m \cos\left[m(\theta - \phi_{no})\right]. \tag{23}$$

For the $m = 2$ mode, the minimum number of the PZT elements required for either the cosine or the sine modal actuator is 4 ($N = 2$ m). Substituting for N into Eq. (20) gives

$$W^c = V^c \sum_{p_z=0}^{N-1} \sum_{n=0}^{\infty} A_n \cos(n\theta) \cos\left(\pi p_z \frac{n}{m}\right) [\cos(\pi p_z)]. \tag{24}$$

Using the property of orthogonality, the above equation becomes

$$W^c = N V^c [A_m \cos(m\theta) + A_{3m} \cos(3m\theta) + A_{5m} \cos(5m\theta) + \cdots]. \tag{25a}$$

This shows clearly that for the desired mode of $m = 2$ with four PZT elements the cosine modal actuator excites the pipe modes $n = 2, 6$ and so on. The sine modal actuator for the $m = 2$ mode is also obtained by similar analysis and is given by

$$W^s = N V^s [A_m \sin(m\theta) + A_{3m} \sin(3m\theta) + A_{5m} \sin(5m\theta) + \cdots]. \tag{25b}$$

The total radial response can be determined by combining Eqs. (25a) and (25b) and substituting V^c and V^s to give

$$W^{tot} = N V^{tot} \left\{A_m \cos[m(\theta - \phi_{no})] + A_{3m} \cos[m(3\theta - \phi_{no})] + A_{5m} \cos[m(5\theta - \phi_{no})] + \cdots\right\}. \tag{26}$$

4. Experimental work

An experiment was carried out to validate the transfer function of a single PZT element and subsequent experiments were conducted to validate the theoretical model of the modal actuator. The objective was to develop a modal actuator for the $n = 2$ mode using the smallest number of PZT elements possible without causing significant spillover to the higher modes of the pipe. Thus, the minimum number of PZT elements for the modal actuator was used and its effectiveness evaluated.

A schematic of the experimental set up to measure the transfer function for a single PZT element is shown in Fig. 3, in which one PZT element was used rather than a set of PZT elements. Since the 5.5 m long pipe, whose properties are given in Table 1, was assumed to have infinite length (which means there are no reflected waves from the ends of the pipe), anechoic terminations in the form of sand boxes were fixed at both ends of the pipe. Each PZT element was manufactured by Morgan Matroc Limited with the shape of a rectangular plate of $4 \times 8 \times 0.25\,\text{mm}^3$. Some important properties of the elements are listed in Table 2, which were used in the prediction of the pipe response. The PZT element was bonded on the pipe at a position equidistant from both anechoic terminations. A random signal voltage from an HP 3566A Signal

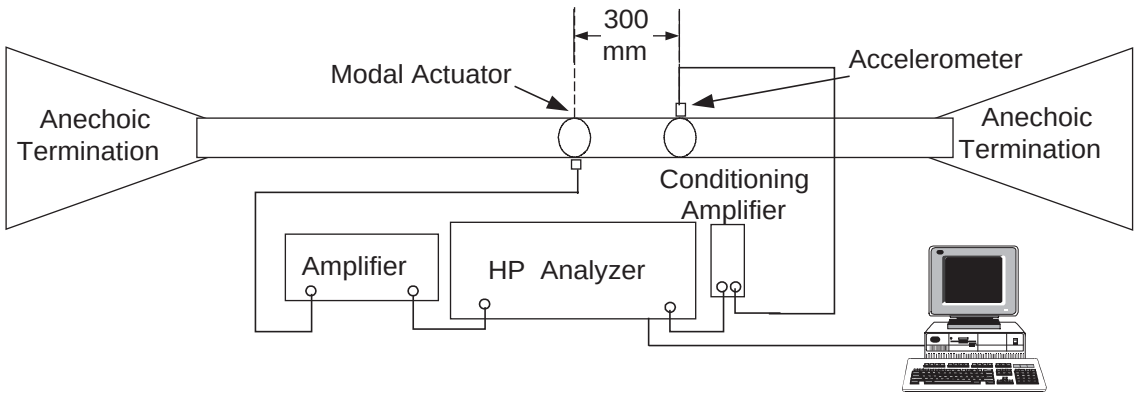

Fig. 3. Experimental set-up for evaluation of the modal actuator for the $n = 2$ mode of the pipe (or a single PZT element).

Table 1
Properties of a PVC pipe

E (N/m^2)	ρ (kg/m^3)	v	a (mm)	h (mm)	η
3.974×10^9	1460	0.33	33.2	2.2	0.035

Table 2
Properties of a PZT element (Morgan Matroc [1]) used for modal actuators

E_z (N/m^2)	ρ_z (kg/m^3)	v_z	d_{31} (m/V)	h_z (mm)
61×10^9	7450	0.31	274×10^{-12}	0.25

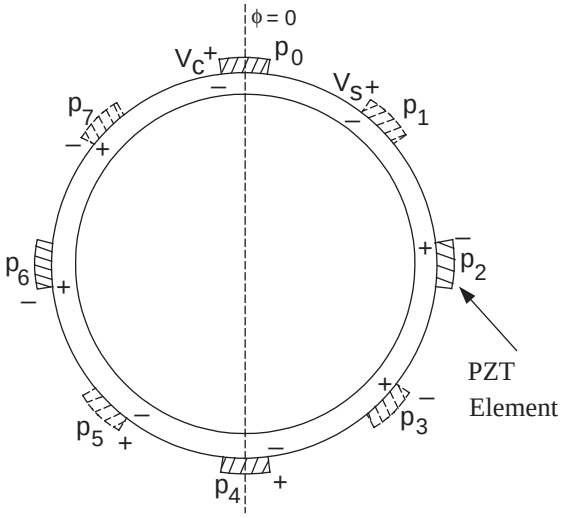

(a)

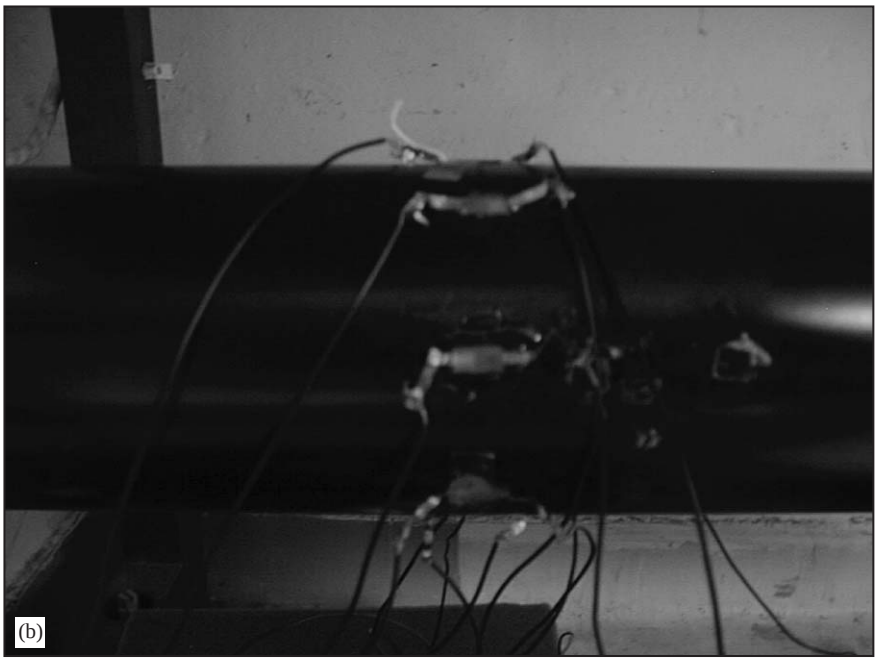

Fig. 4. Arrangement of the $n = 2$ PZT modal actuators; (a) Diagram, — cosine function actuator, – – sine function actuator, (b) photograph.

Analyzer was supplied to the PZT element via a power amplifier. The resulting motion of the pipe was measured at the distance of 300 mm from the position of the PZT element by an accelerometer moved to 32 positions located around the pipe. The radial motion could thus be decomposed into each mode of the pipe using the method of modal decomposition, which is

described later. Hence, the expression for the transfer function of a single PZT element bonded to the pipe could be evaluated by comparing it with the experimental results for each mode.

An experiment was also carried out to validate the model for the $n = 2$ modal actuator. Eight PZT elements were bonded to the pipe as shown in Fig. 4 (four elements for the sine modal actuator and other four elements for the cosine modal actuator). As described in the previous section, the voltage supplied to the PZT elements for the cosine modal actuator has to be varied as the cosine function of $V_r^c = V^c \cos(2\pi m(p_z/N))$. Hence, only the PZT elements at the positions of $p = 0$, 2, 4 and 6 were activated with $+V^c$, $-V^c$, $+V^c$, $-V^c$, respectively, while those at the other positions had zero input voltage. Similar to the cosine modal actuator, the sine modal actuator required the voltage to be supplied to the elements at positions of $p = 1$, 3, 5 and 7 with $+V^s$, $-V^s$, $+V^s$, $-V^s$, respectively, while those at the other positions had zero input voltage. The radial motion of the pipe was excited by the cosine modal actuator and the measurement method was similar to that of the transfer function for the single PZT element. Finally, to explore the change of the orientation angle, both sine and cosine modal actuators were simultaneously actuated first with the same magnitude of input voltage and secondly with the input voltage of the sine modal actuator equal to half of that of the cosine modal actuator.

To compare the predictions with the experimental results, the complex elastic modulus of the pipe, $E' = E(1 + j\eta)$ where η is the loss factor, was used to take account of structural damping. The static gains of each PZT element g_q (for forces) and g_q (for moments), which were used to calculate the response of the pipe, are given by [15]

$$g_q = \frac{\alpha^2(1 + \mu\tau\alpha^3)}{1 + \mu\tau\alpha(4 + 6\alpha + 4\alpha^2 + \mu\tau\alpha^3)}\gamma d_{31},$$

$$g_m = \frac{\alpha^2(1 + \alpha)}{2[1 + \mu\tau\alpha(4 + 6\alpha + 4\alpha^2 + \mu\tau\alpha^3)]}h\gamma d_{31},$$

where

$$\alpha = h_z/h, \quad \psi = \frac{1 - \nu^2}{1 - \nu_z^2}\frac{E_z}{E}, \quad \mu = \frac{1 - \nu}{1 - \nu_z}, \quad \tau = \frac{E_z}{E} \text{ and } \gamma = \frac{E_z}{1 - \nu_z}$$

h_z, E_z and ν_z are thickness, Young's modulus and Poisson ratio of each PZT element.

To compare the response for a single mode, the modal decomposition technique described by the authors [21] was applied to a set of measured frequency responses to give the amplitude of the transfer function, A_d, and the reference angle, ϕ

$$A_d = \frac{1}{N_m}\sqrt{\left[\frac{1}{N_m}\sum_{p_\theta=0}^{N_m-1} T_{p_\theta}\cos\left(\frac{2\pi p_\theta}{N_m}d\right)\right]^2 + \left[\frac{1}{N_m}\sum_{p_\theta=0}^{N_m-1} T_{p_\theta}\sin\left(\frac{2\pi p_\theta}{N_m}d\right)\right]^2},$$

$$\phi = \frac{1}{d}\tan^{-1}\left(\frac{\frac{1}{N_m}\sum_{p_\theta=0}^{N_m-1} T_{p_\theta}\sin\left(\frac{2\pi p_\theta}{N_m}d\right)}{\frac{1}{N_m}\sum_{p_\theta=0}^{N_m-1} T_{p_\theta}\cos\left(\frac{2\pi p_\theta}{N_m}d\right)}\right),$$

where d is the mode of interest, p_θ is the position of the measurement, N_m is the number of measurements around the pipe and T_{p_θ} is the measured transfer mobility at the position p_θ.

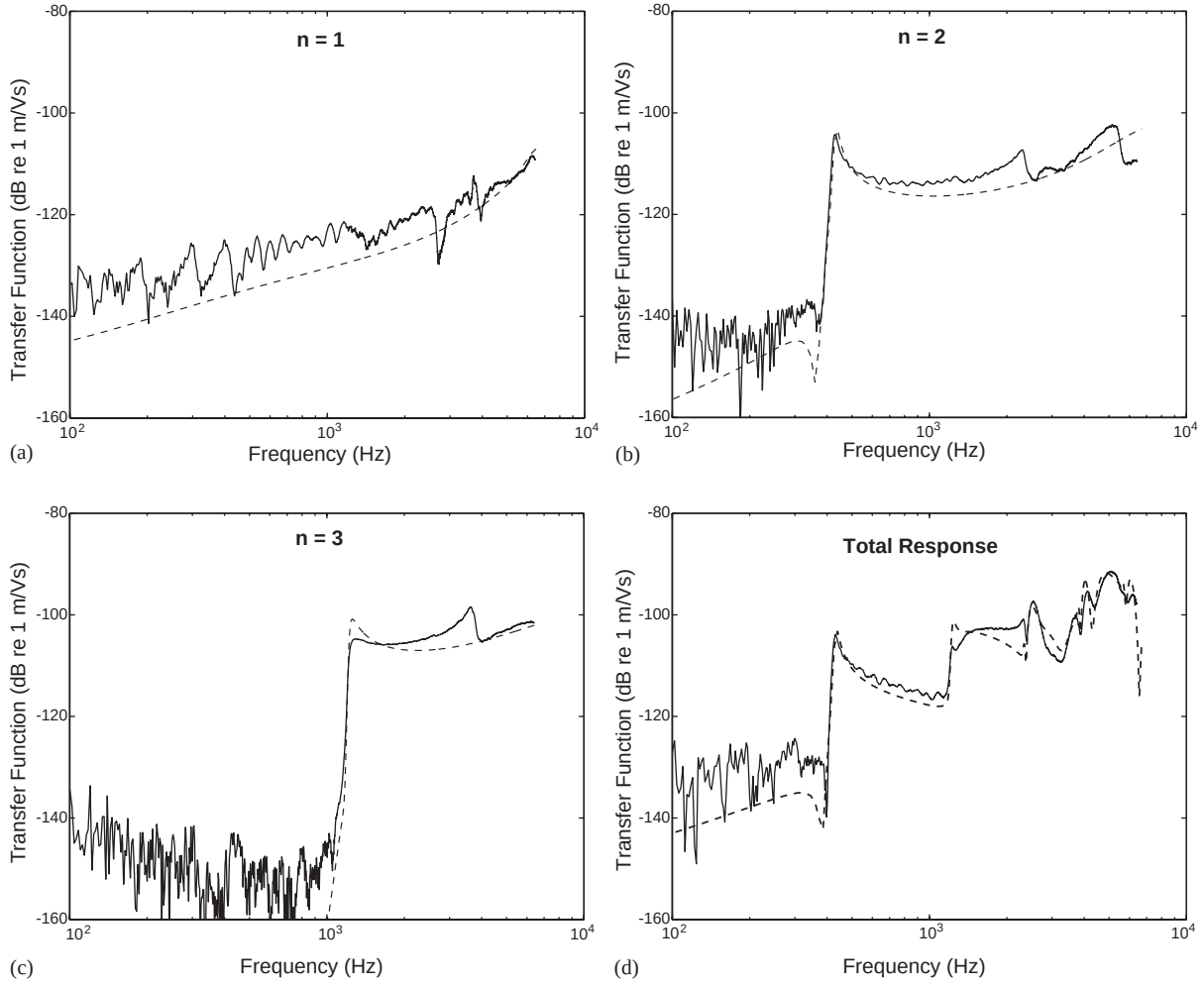

Fig. 5. Amplitude of the transfer function of the pipe for the $n = 1-3$ modes and all modes, which are excited by a single actuator;---- prediction (Eq. (17)), — measurement.

It should be noted that the modal decomposition method was not effective for the $n = 0$ mode because of the very small motion of the pipe Ref. [21]. Examination of Fig. 5 shows that for the $n = 1-3$ modes and the combination of all modes, the predictions of the behaviour of the pipe excited from a single PZT element are consistent with practice except at low frequencies, where the motion of the pipe is very small.

As mentioned earlier, the elements of the cosine modal actuator require the input voltage as $+V^c$, $-V^c$, $+V^c$, $-V^c$, at an angle of 0, $\pi/2$, π, $3\pi/2$, respectively. With such an input voltage, the response of the $n = 2$ mode of the pipe is strengthened and that of the other modes is cancelled as shown in Fig. 6. The very small response of the $n = 4$ mode can be seen clearly in Fig. 6a. Excitation of the $n = 6$ mode, which is spillover due to there being insufficient elements in the modal actuator, was also expected to be excited, and appears in Fig. 6, but the response measured is less than that predicted. This is probably because of the effect of the mass loading from the

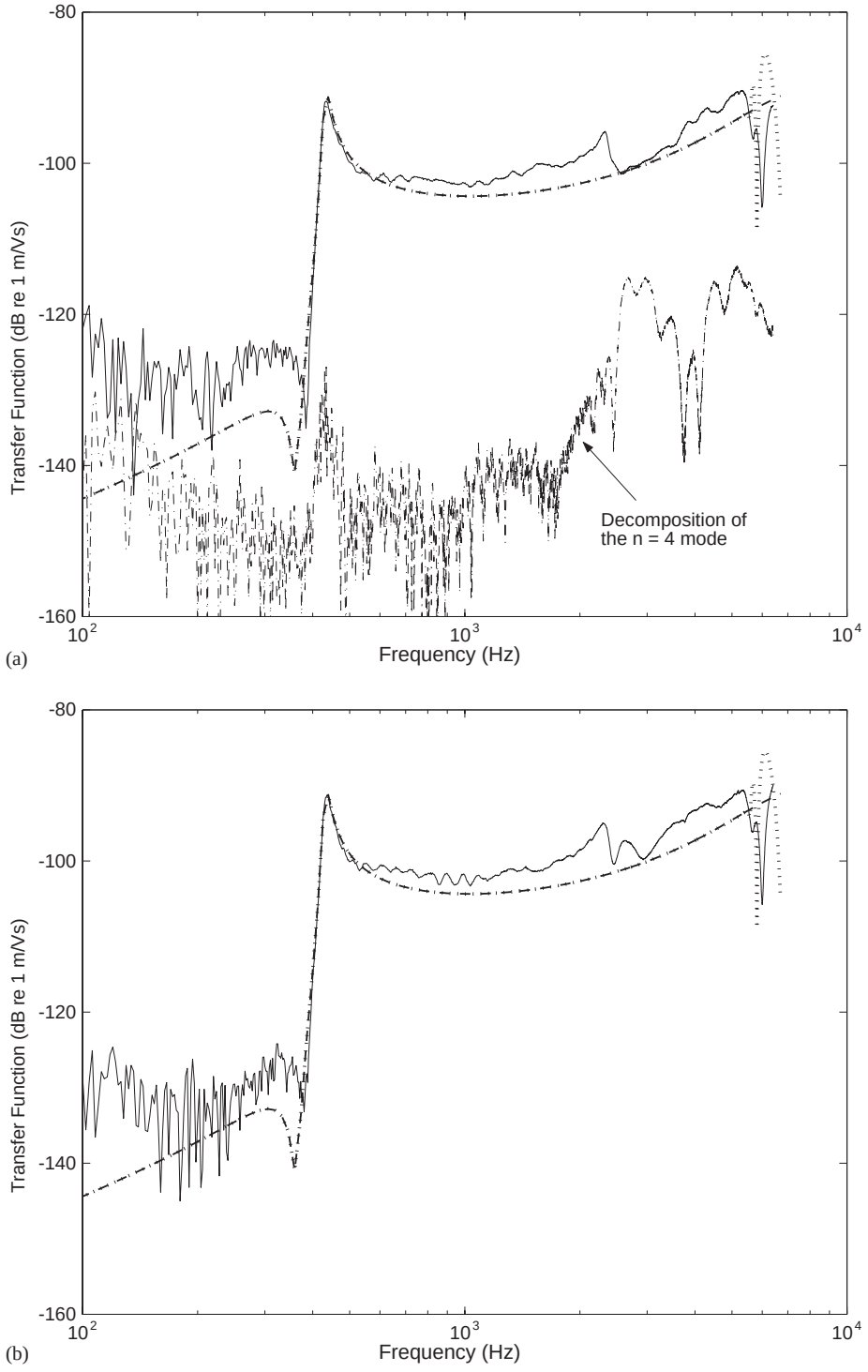

Fig. 6. Amplitude of the transfer function of the pipe; — Measurement, – – only the $n = 2$ mode; … combination of the $n = 2$ and $n = 6$ modes; –·– response of decomposing the $n = 4$ mode; (a) The $n = 2$ cosine modal actuator, (b) the $n = 2$ sine modal actuator.

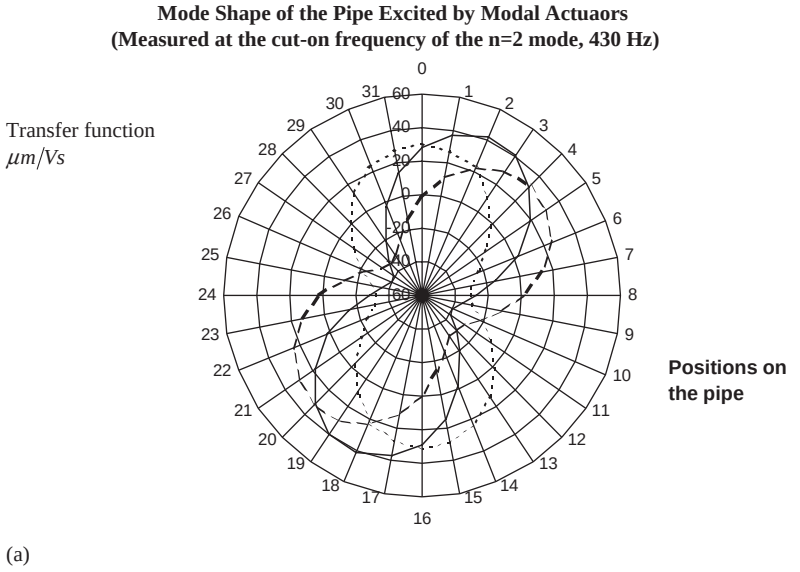

(a)

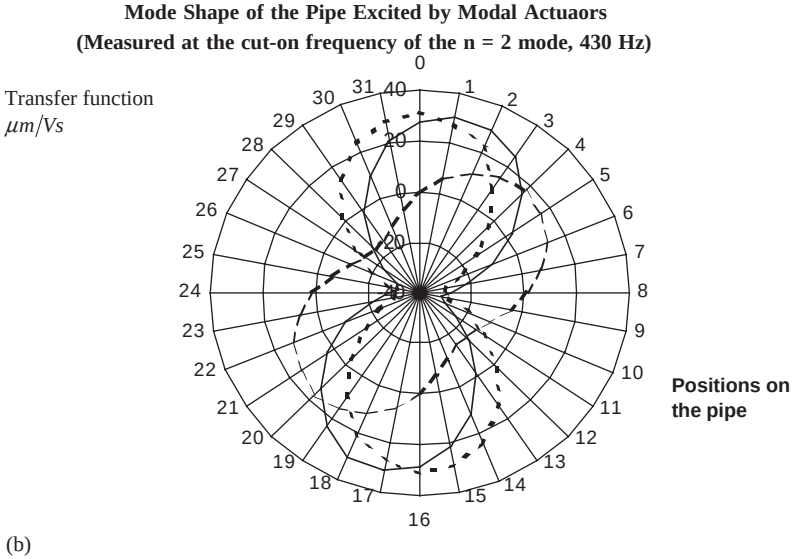

(b)

Fig. 7. Orientation angle of the pipe arising from the excitation of both modal actuators; ··· cosine, – – sine, — both; (a) the same amplitude of the input voltage; (b) the input voltage of the sine modal actuator equal to half that of the cosine modal actuator.

accelerometers as discussed in Ref. [21]. The effect of this spillover occurs at the relatively high frequency of 5532 Hz for the $n = 6$ mode, and so may be ignored. It can be seen in Fig. 6 that there is reasonably good agreement between practice and theory.

The change in the orientation angle when using both sine and cosine modal actuators can be seen in Fig. 7. With the same voltage supplied to both modal actuators, the predicted angle is $\phi = 22.5$ degrees, while it is $\phi = 13.3$ when the input voltage of the cosine modal actuator is twice of that of the sine modal actuator.

5. Conclusions

Expressions for the radial motion of a pipe excited by a single PZT actuator, and sine and cosine modal actuators for the $n = 2$ mode have been derived. They have also been successfully validated by experiment. It has been shown that a sine or cosine modal actuator for this mode can be created by using only four PZT elements, which is the minimum number for such an actuator. With this number of PZT elements, spillover of the $n = 6$ mode occurs. However, it has been shown that this may be largely neglected because it occurs at a high frequency.

When both modal actuators are used, the orientation angle of the response with respect to the cosine modal actuator can be controlled. By exploring the mode shape of the pipe generated by both actuators simultaneously, it has been shown that the orientation angle of the pipe can be readily adjusted by controlling their input voltage.

Appendix A. Simplified wavenumbers

This appendix summarizes the simplified low frequency wavenumbers (poles) reported by Variyart and Brennan [14].

For the $n = 0$ mode,

$$\hat{k}_{01}^2 = \hat{k}_l^2, \quad \hat{k}_{02}^2 = \hat{k}_s^2, \quad \hat{k}_{03}^2, \hat{k}_{04}^2 = \pm \mathrm{j}\sqrt{(1-\nu^2)(1-\hat{k}_l^2)/\beta^2}. \tag{A.1}$$

For the $n = 1$ mode,

$$\hat{k}_{11}^2, \hat{k}_{12}^2 = \frac{1}{2(1-\hat{k}_l^2)}\left[(1-\hat{k}_l^2)(\hat{k}_l^2+\hat{k}_s^2) + \hat{k}_b^4 \pm 2\hat{k}_b^2\right],$$

$$\hat{k}_{13}^2, \hat{k}_{14}^2 = \pm \mathrm{j}\sqrt{(1-\nu^2)(1-\hat{k}_l^2)/\beta^2}. \tag{A.2}$$

For the $n \geqslant 2$ modes

$$\hat{k}_{n1}^2 = \frac{n^2[(\Omega^2 - 2\Omega_{co}^2) + \sqrt{(1-\nu^2+3\Omega_{co}^2)(\Omega^2-\Omega_{co}^2)+\Omega_{co}^4}]}{\beta^2 \hat{k}_{n3}^2 \hat{k}_{n4}^2},$$

$$\hat{k}_{n2}^2 = \frac{n^2\left[(\Omega^2 - 2\Omega_{co}^2) - \sqrt{(1-\nu^2+3\Omega_{co}^2)(\Omega^2-\Omega_{co}^2)+\Omega_{co}^4}\right]}{1-\nu^2-\Omega^2+6\Omega_{co}^2}, \tag{A.3}$$

$$\hat{k}_{n3,n4}^2 = -n^2 + \frac{1}{6}\left[-\left(3z^{1/3} - \frac{(1-\nu^2-\Omega^2)}{\beta^2 z^{1/3}}\right) \pm \mathrm{j}\sqrt{3}\left(3z^{1/3} + \frac{(1-\nu^2-\Omega^2)}{\beta^2 z^{1/3}}\right)\right],$$

where

$$z = \left(\frac{1-\nu^2}{\beta^2}\right)\left[1 + \sqrt{1 + \frac{(1-\nu^2-\Omega^2)^3}{27(1-\nu^2)^2\beta^2 n^4}}\right]n^2, \quad \Omega_{co}^2 = \frac{\beta^2 n^2 (n^2-1)^2}{n^2+1},$$

is the cut-on frequency of the pipe

$$\hat{k}_l^2 = \frac{\Omega^2}{1-\nu^2}, \quad \hat{k}_s^2 = \frac{2\Omega^2}{1-\nu}, \text{ and } \hat{k}_b^4 = \frac{2\Omega^2}{(1+3\beta^2)(1\text{-}\nu^2)} \cong 2\hat{k}_l^2$$

are the non-dimensional wavenumbers of longitudinal, torsional and flexural bending waves of a pipe normalized to its radius.

References

[1] Morgan Matroc Limited Piezoelectric ceramics: Data book for designers. Transducer products division, Morgan Matroc Limited, Bewdley Road, Stourport-on-Severn, Worcestershire, DY13 8QR.

[2] M. Balas, Feedback control of flexible systems, IEEE Transactions on Automatic Control AC-23 (4) (1978) 673–679.

[3] S.E. Burke, J.E. Hubbard Jr., Distributed transducer vibration control of thin plates, Journal of the Acoustical Society of America 90 (1991) 937–944.

[4] C.K. Lee, Theory of laminated piezoelectric plates for the design of distributed sensors/actuators. Part I: governing equations and reciprocal relationships, Journal of the Acoustical Society of America 87 (1990) 1144–1158.

[5] C.K. Lee, F.C. Moon, Modal sensors/actuators, Journal of Applied Mechanics 57 (1990) 434–441.

[6] H.S. Tzou, Anew distributed sensor and actuator theory for intelligent shells, Journal of Sound and Vibration 153 (1992) 335–349.

[7] C.K. Sung, T.F. Chen, S.G. Chen, Piezoelectric modal sensor/actuator design for monitoring/generating flexural and torsional vibrations of cylindrical shells, Journal of Vibration and Acoustics 118 (1996) 48–55.

[8] M.J. Brennan, M.J. Day, S.J. Elliott, R.J. Pinnington, Piezoelectric actuators and sensors, Proceedings of IUTAM Symposium on Active Control of Vibration, Bath, England, 1994, pp. 263–274.

[9] J. Tani, J. Qiu, H. Miura, Vibration control of a cylindrical shell using piezoelectric actuators, Journal of Intelligent Material Systems and Structures 6 (1995) 380–388.

[10] J. Qiu, J. Tani, Vibration control of a cylindrical shell using distributed piezoelectric sensors and actuators, Journal of Intelligent Material Systems and Structures 6 (1995) 474–481.

[11] H.C. Lester, S. Lefebvre, Piezoelectric actuator models for active sound and vibration control of cylinders, Proceedings of Recent Advances in Active Control of Sound and Vibration, Blacksburg, VA, 1991. pp. 3–26.

[12] F. Lalande, Z. Chaudhry, C.A. Rogers, Impedance-based modeling of actuators bonded to shell structures, SPIE Conference on Smart Structures and Materials, San Diego, CA 2443, 1995, pp. 396–408.

[13] C.R. Fuller, F.J. Fahy, Characteristics of wave propagation and energy distributions in cylindrical elastic shells filled with fluid, Journal of Sound and Vibration 81 (1982) 501–518.

[14] W. Variyart, M.J. Brennan, Simplified dispersion relationships for in-vacuo pipes, Journal of Sound and Vibration 256 (5) (2002) 955–967.

[15] W. Variyart, Ph.D. Thesis, University of Southampton, Southampton, Active Control of Flexural Waves in In-vacuo Pipes, 2001.

[16] A.W. Leissa, Vibrations of shells, NASA SP-288, US Government Printing Office, Washington, DC, 1973.

[17] W. Flügge, Stresses in Shells, 2nd Edition, Springer-Verlag, Berlin, Heidelberg, New York, 1962.

[18] C.F. Fuller, The input mobility of an infinite circular cylindrical elastic shell filled with fluid, Journal of Sound and Vibration 87 (1983) 409–427.

[19] E.K. Dimitriadis, C.R. Fuller, C.A. Rogers, Piezoelectric actuators for distributed vibration excitation of thin plates, Journal of Vibration and Acoustics 113 (1991) 100–107.

[20] G. Arfken, Mathematical Methods for Physicists, 3rd Edition, Academic Press, New York, 1985.

[21] M.J. Brennan, W. Variyart, Simplified mobility expressions for infinite in-vacuo pipes, Journal of Sound and Vibration 260 (2) (2003) 329–348.